Electrically tunable quantum anomalous Hall effect in graphene decorated by 5d transition-metal adatoms. — Source link ⬈

Hongbin Zhang, Cesar Lazo, Stefan Blügel, Stefan Heinze ...+1 more authors

Institutions: Forschungszentrum Jülich, University of Kiel

Topics: Quantum anomalous Hall effect, Quantum Hall effect, Quantum spin Hall effect, Spin Hall effect and Graphene

Related papers:

- Generalized Gradient Approximation Made Simple

- Quantum anomalous Hall effect in graphene from Rashba and exchange effects

- Experimental Observation of the Quantum Anomalous Hall Effect in a Magnetic Topological Insulator

- Efficient iterative schemes for ab initio total-energy calculations using a plane-wave basis set.

- Quantized Anomalous Hall Effect in Magnetic Topological Insulators

Share this paper: 🇫 🇹 in ✉

Electrically Tunable Quantum Anomalous Hall Effect in Graphene Decorated by 5d Transition-Metal Adatoms

Hongbin Zhang,[1,*] Cesar Lazo,[2] Stefan Blügel,[1] Stefan Heinze,[2] and Yuriy Mokrousov[1]

[1]*Peter Grünberg Institut and Institute for Advanced Simulation, Forschungszentrum Jülich and JARA, D-52425 Jülich, Germany*
[2]*Institute of Theoretical Physics and Astrophysics, University of Kiel, D-24098 Kiel, Germany*
(Received 24 September 2011; published 1 February 2012)

Based on first-principles calculations, we predict that 5d transition metals on graphene present a unique class of hybrid systems exhibiting topological transport effects that can be manipulated effectively by external electric fields. The origin of this phenomenon lies in the exceptional magnetic properties and the large spin-orbit interaction of the 5d metals leading to significant magnetic moments accompanied with colossal magnetocrystalline anisotropy energies. A strong magnetoelectric response is predicted that offers the possibility to switch the spontaneous magnetization direction by moderate electric fields, enabling an electrically tunable quantum anomalous Hall effect.

The spin-orbit interaction couples the spin degree of freedom of electrons to their orbital motion in the lattice. This leads to many prominent physical phenomena [1–3] in conventional ferromagnets. It is also the key interaction in the newly found quantum topological phase in topological insulators, where the quantum spin Hall effect was observed experimentally [4], and the quantum anomalous Hall effect (QAHE) was predicted to exist [5,6]. Since the orbital motion can be manipulated with external electric fields, spin-orbit coupling (SOC) opens a route to electrical control of magnetic properties [7–9], playing a crucial role in future spintronics applications.

Owing to their strong spin-orbit coupling, heavy 4d and 5d transition-metals (TMs) display fascinating physical properties for desirable spintronic applications, especially when combined with a nonvanishing magnetization. However, magnetism of 5d TMs proved difficult to achieve, even for low-dimensional structures [10–12], because their valence d wave functions are more delocalized than those of Fe, Co, and Ni. Moreover, the interfacial diffusion and strong d-d hybridization suppress magnetism upon the deposition of 5d TMs on commonly used noble-metal substrates. From this point of view, using sp substrates is more promising. In fact, 4d ferromagnetism was first observed in a Ru monolayer deposited on the graphite (0001) surface [13], which is close to graphene in its chemical and physical properties.

Since the day graphene was isolated and produced as a two-dimensional material [14,15], it abruptly altered the research direction of nanoelectronics with the aim of exploring its fascinating transport properties. In a sense, graphene serves as a prototype of the topological insulators [16]. For instance, the Berry phase of π of electronic states in graphene induces a half-integer quantum Hall effect [17,18], and the existence of the quantum spin Hall effect was first suggested for pure graphene after the SOC has been considered [19]. One common feature for those transport properties is the nontrivial topological origin, resulting in dissipationless charge or spin current carried by edge states with conductivity quantized in units of e^2/h. However, from the application point of view, a large external magnetic field is required to obtain the quantum Hall effect, and the spin degeneracy in the quantum spin Hall effect makes it hard to manipulate the spin degree of freedom by controlling external fields. To avoid such constraints while keeping the benefit of topologically protected quantized transport, the long-sought QAHE could be a perfect solution. The essence of the QAHE lies in the quantization of the transverse charge conductivity in a material with intrinsic nonvanishing magnetization. The fact that the magnetization in ferromagnets can be manipulated experimentally much easier than large magnetic fields in dia- or paramagnets makes the QAHE extremely attractive for applications in spintronics and quantum information. However, at present the QAHE is merely a generic theoretical concept for magnetically doped topological insulators [5,6]. Recently, Qiao *et al.* suggested that the QAHE could also occur at comparatively low temperatures in graphene decorated with Fe adatoms [20].

Here, we demonstrate based on first-principles theory that 5d TMs deposited on graphene are strongly magnetic, provide colossal magnetocrystalline anisotropy energies (MAE) and exhibit a strong magnetoelectric response as well as topologically nontrivial band gaps, all due to very strong spin-orbit interaction. A generic representative of this hybrid class of materials has a magnetocrystalline anisotropy energy of 10–30 meV per TM, a magnetoelectric response of 6–30 G · nm²/V, and a quantum anomalous Hall gap of 20–80 meV. In connection with the large magnetoelectric response of the deposited adatoms, we predict that the magnetization direction can be switched between in-plane and out-of-plane directions by applying a moderate external electric field, thus resulting in an

electrically tunable QAHE, which could be observed experimentally at room temperature.

We have performed first-principles calculations of 5d TM (Hf, Ta, W, Re, Os, Ir, and Pt) adatoms on graphene in 2×2, 3×3, and 4×4 supercell geometries corresponding to the deposition density of 4.7, 2.1, and 1.2 atoms/nm^2, respectively, (see Supplemental Material [21] for details). Throughout this work the TM atoms are placed at the hollow sites of graphene. According to previous theoretical studies [22], it is the most favorable adsorption site except for Pt [23] and Ir [24], for which the bridge site is preferred. Among all systems studied we discuss at first the adatoms with 4×4 superstructure and we selected one prototype system, W on graphene, that we discuss in more detail. In the 4×4 geometry, the optimized distance between W adatoms on the hollow site and the C plane is about 1.74 Å, and the hollow site is about 0.14 eV (0.41 eV) per TM atom lower in energy than the bridge (top) site, in agreement with previous observations [25]. Applying an electric field, the relaxed positions change by at most 0.01 bohr, and the hollow site remains the preferred adsorption site.

From our calculations, we conclude that all 5d TMs (except for Pt and 2×2 Hf and Os) are magnetic, with sizable magnetic moments ranging between 0.5 and $2\mu_B$. Unique to the 5d TMs is the property that the SOC and the intra-atomic exchange are of the same magnitude, which is manifested by the colossal values of the MAE, defined as the total-energy difference between the magnetic states with spin moments aligned in the plane and out of the graphene plane directions. For the systems considered, the calculated MAEs are very large, typically in the range of 10–30 meV per TM (see Supplemental Material [21]). The MAE presents one of the most fundamental quantities of any magnetic system as its sign defines the easy magnetization axis and its magnitude provides an estimate of how stable the magnetization is. A large MAE makes the magnetization stable but also difficult to manipulate.

Since graphene is quite responsive to external electric fields [15,26], we have investigated how far the magnetic properties of these hybrid systems can be manipulated by applying electric fields. In Fig. 1, we show the dependence of the spin moments and the MAE of W adatoms in 4×4 geometry as a function of the electric field $\mathcal{E}$, applied perpendicularly to the graphene layer (along the z axis). Remarkably, the spin moment of W displays a strong dependence on the field strength, especially when the magnetization points out of plane. Qualitatively, this response can be characterized by a magnetoelectric coefficient α, which relates the change of the tungsten spin moment $\Delta\mu_S$, to the strength of the $\mathcal{E}$ field: $\mu_0\Delta\mu_S = \alpha\mathcal{E}$, where μ_0 is the vacuum magnetic permeability constant. For W adatoms on graphene and an out-of-plane magnetization, $\alpha_\perp(W)$ amounts to about 30 G · nm^2/V, which is 1 order of magnitude larger than that in Fe thin
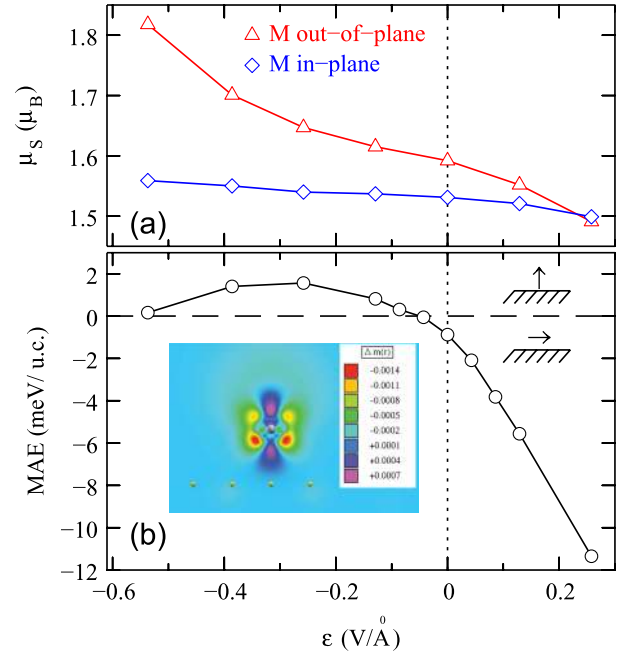

FIG. 1 (color online). Dependence of the spin magnetic moments of W adatoms μ_S (in μ_B) for the out-of-plane and in-plane magnetization (a) and magnetic anisotropy energy MAE (b) as a function of the external electric field $\mathcal{E}$. The electric field applied is perpendicular to graphene surface, with negative values of $\mathcal{E}$ corresponding to the electric field in $+z$ direction, i.e., the direction from graphene towards the adatoms. Positive (negative) MAE corresponds to an out-of-plane (in-plane) easy axis. The inset displays the difference between spin densities $\Delta m(r)$ (in units of electrons/a.u.^{3}) for the system without and with an electric field of -0.13 V/Å.

films [8]. For an in-plane magnetization, the magnetoelectric coefficient $\alpha_\|(W)$ is only 6 G · nm^2/V, i.e., 1 order of magnitude smaller than $\alpha_\perp(W)$, which underlines the strong anisotropy of this quantity. We observe similarly large variations of the magnetoelectric strength in other considered 5d TMs. In difference to the spin moment, the dependence of the orbital moment with respect to the $\mathcal{E}$ field is negligible for all systems.

Striking is the effect of the electric field on the magnetization direction [see Fig. 1(b)]. At zero field ($\mathcal{E} = 0$) the magnetization is in plane. Applying negative fields of magnitude between 0.05 and 0.4 V/Å, values typical in graphene field effect transistor structures [27], the sign of the MAE is changed. This means that the equilibrium direction of the magnetization can be switched from in-plane (MAE < 0, for $\mathcal{E} = 0$) to out-of-plane (MAE > 0 for $\mathcal{E} < 0$). Supposing that the $\mathcal{E}$ field is completely screened in our system by forming a screening charge δq, the variation of the MAE with respect to δq, δMAE/δq, reaches as much as 28 meV/e for negative electric fields, which is more than 3 times larger than the one at the surface of CoPt slabs [28], and 1 order of magnitude larger than that of Fe slabs [8]. With a moderate out-of-plane electric field of

± 0.13 V/Å switching of the magnetization can also be achieved for Hf adatoms, and the MAE can be significantly altered in Os (by ≈ 10 meV) and Ir on graphene (by ≈ 20 meV). This establishes the $5d$ TM adatoms on graphene as a novel class of hybrid materials with high susceptibility of the magnetic properties in terms of an electric field, thus making the electrical control of magnetism possible in these systems.

An understanding is provided on the basis of the local tungsten s- and d-decomposed density of electron states without SOC, grouped into $\Delta_1(s, d_{z^2})$, $\Delta_3(d_{xz}, d_{yz})$, and $\Delta_4(d_{xy}, d_{x^2-y^2})$ contributions, presented in Fig. 2(a). As we can see, the W spin moment of about $1.6\mu_B$ originates from two occupied spin-up and two unoccupied spin-down Δ_1 states, while the exchange-split Δ_3 and Δ_4 states are situated above and below E_F, respectively, and almost do not contribute. Upon including SOC (e.g., for out-of-plane spins) a strong hybridization between the $\Delta_1^\downarrow$, and Δ_3 and

Δ_4 states of both spin occurs around E_F [see also Fig. 2(b)], which results in a formation of hybrid bands of mixed spin and orbital character [see Fig. 2(c)]. When an electric field is applied along the z axis, the $\Delta_1^\uparrow$ states experience the greatest influence of the corresponding potential change as they are directed perpendicularly to the graphene plane. Corresponding modifications of the band structures can be seen in Fig. 2(c), where the $\Delta_1^\uparrow$ band is shifted downwards (upwards) by negative (positive) applied $\mathcal{E}$ fields, while the hybrid bands of mixed character remain almost unaffected. This causes the redistribution of the electrons in the $\Delta_1^\uparrow$ states by its hybridization with the hybrid bands below the Fermi level, hence the variation of the magnetic moment. This is visualized by the spin-density difference plotted in the inset in Fig. 1(b). It is obvious that, upon applying an electric field, a certain amount of spin density is transferred from the d_{z^2} character of the Δ_1 state to the Δ_3 states. Owing to the difference in the hybridization with
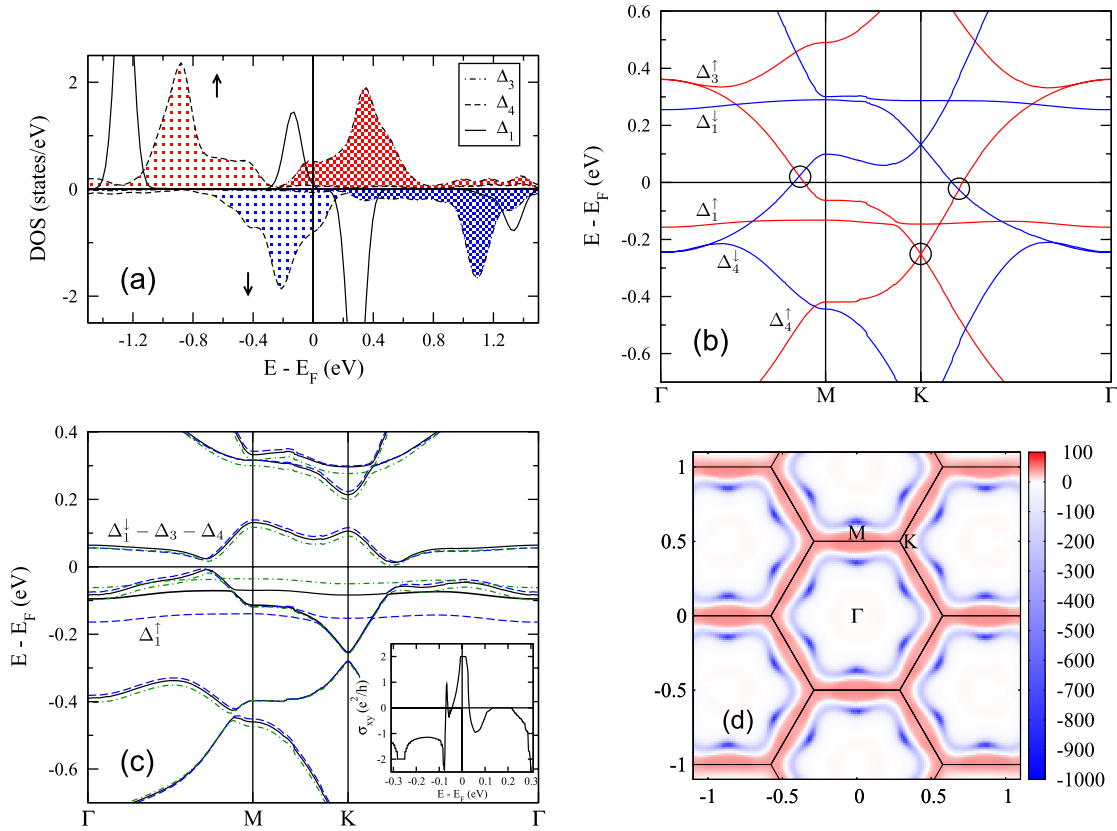

FIG. 2 (color online). Electronic structure of 4×4 W on graphene. (a) Density of $\Delta_1(s, d_{z^2})$, $\Delta_3(d_{xz}, d_{yz})$, and $\Delta_4(d_{xy}, d_{x^2-y^2})$ states without SOC. Up and down arrows mark spin-up (red) and spin-down (blue) channels, respectively. Δ_3 [Δ_4] states are located predominantly above [below] the Fermi energy, and are shaded in line-shaded dark red (light gray) or blue (dark gray) [dot-shaded red (light gray) or blue (dark gray)] correspondingly. (b) Band structure without SOC along high symmetry lines in the 2D Brillouin zone. Red and blue color of the bands stands for the spin-up and spin-down character, respectively. Circles highlight the points at which a gap will open when SOC is considered. (c) Band structures with SOC for **M** $\parallel z$: without electric field (solid line), with positive (dashed) and negative (dot-dashed) electric field of magnitude 0.13 V/Å. The inset shows the anomalous Hall conductivity with respect to the position of the Fermi energy E_F for $\mathcal{E} = 0$ and **M** $\parallel z$. (d) Berry curvature (in units of a.u.²) distribution of occupied bands in the momentum space (in units of $\frac{2\pi}{a}$, where $a = 9.87$ Å is the in-plane lattice constant of the 4×4 supercell). The Brillouin zone boundaries are marked with solid lines.

the graphene states, seen from the width of the corresponding peaks in the density of states [Fig. 2(a)], the Δ_1 and Δ_3 states have different localization inside the W atoms thus explaining the change in the spin moment. In turn, the details of hybridization between the W d states depend sensitively on the magnetization direction via the spin-orbit matrix elements [29], resulting in a strong anisotropy of the magnetoelectric response, observed in Fig. 1(a).

At last we turn to the central point of the Letter, that is a prediction of a stable QAHE, a manifestation of the quantization of the transverse anomalous Hall conductivity. It is motivated by the observation that for W adatoms on graphene with an out-of-plane magnetization, Δ_3 and Δ_4 bands of opposite spin cross at E_F [see circles in Fig. 2(b)] and hybridize under the presence of SOC, forming a global band gap across the Brillouin zone (BZ). Thus, the W-graphene hybrid system becomes an insulator upon a spin-orbit driven metal-insulator transition. We compute the anomalous Hall conductivity of this system, given by $\sigma_{xy} = (e^2/h)\mathcal{C}$, where $\mathcal{C}$ is the Chern number of all occupied bands that can be obtained by a k-space integral $\mathcal{C} = \frac{1}{2\pi} \int_{BZ} \Omega(\mathbf{k}) d^2 k$. The integrand $\Omega(\mathbf{k})$ is the so-called Berry curvature of all states below the Fermi level:

$$\Omega(\mathbf{k}) = \sum_{n<E_F} \sum_{m \neq n} 2\text{Im} \frac{\langle \psi_{n\mathbf{k}} | v_x | \psi_{m\mathbf{k}} \rangle \langle \psi_{m\mathbf{k}} | v_y | \psi_{n\mathbf{k}} \rangle}{(\varepsilon_{m\mathbf{k}} - \varepsilon_{n\mathbf{k}})^2}, \quad (1)$$

where $\psi_{n\mathbf{k}}$ is the spinor Bloch wave function of band n with corresponding eigenenergy $\varepsilon_{n\mathbf{k}}$, v_i is the ith Cartesian component of the velocity operator. The Berry curvature in reciprocal space, presented in Fig. 2(d), displays a comparatively complex pattern, with positive contributions concentrated along the BZ boundary, and large negative dips off the M point. Such a nontrivial distribution of the Berry curvature, which plays the role of an effective magnetic field in the k space, is typical for complex transition-metal compounds [3].

The calculated anomalous Hall conductivity as a function of the electron filling expressed in terms of the energy E relative to the Fermi level E_F is presented in the inset of Fig. 2(c) for an out-of-plane magnetization, $\mathbf{M} \parallel z$, and zero $\mathcal{E}$ field. We indeed find that the Chern number of all occupied states acquires an integer value of $+2$. According to the physics of the quantum Hall effect, this will result in two dissipationless and topologically protected edge states on each side of a finite graphene ribbon with W adatoms. Remarkably, another 32 meV large QAHE gap with the $\mathcal{C} = -2$ can be observed at the energy of -0.27 eV below E_F, originating from the SOC-mediated hybridization between the Δ_3 and Δ_4 bands of the same spin-up character, see Figs. 2(b) and 2(d). Such a peculiar situation suggests that the topological properties, such as the direction of the propagation of the edge states, of the QAHE state in the W-graphene system can be controlled by tuning the position of E_F, e.g., via deposition on an appropriate substrate.

More importantly, at equilibrium the magnetization direction of W lies in-plane, rendering $\sigma_{xy} = 0$ owing to the antisymmetric nature of the anomalous Hall conductivity with respect to the magnetization direction. From our previous discussion it follows, however, that the direction of $\mathbf{M}$ can be conveniently switched to out-of-plane by applying a moderate electric field. In this case the gaps remain intact [cf. Fig. 2(c)], their size unchanged, and the value of the anomalous Hall conductivity remains quantized at both energies.

Such nontrivial topological QAHE states occur also for all other $5d$ adatoms (except Pt) on graphene in 4×4 geometry, and for several of them (Ta, W, Re, and Ir) in 2×2 geometry, with QAHE gaps of comparable magnitude, although not necessarily positioned at the Fermi energy. For example, graphene with Re deposited in 4×4 geometry exhibits three $\mathcal{C} = +2$ QAHE gaps at -1, -0.15, and $+0.67$ eV, with the corresponding gap size of 38, 63, and 98 meV, respectively. Also, for 4×4 Os, there exist two QAHE gaps with $\mathcal{C} = \pm 2$ at -0.38 and 0.15 eV, with corresponding gap sizes of 11 and 80 meV, respectively. The fact that several QAHE gaps with different Chern numbers at different energies can occur in the same material makes these systems a rich playground for topological transport studies. For such systems, the creation of the QAHE gaps occurs not at time-reversal symmetric points of the Brillouin zone, and the gaps are determined by $5d$ orbitals of TMs. This is in contrast to the cases considered previously [5,6,20], in which the role of the magnetic adatoms was rather to introduce Rashba spin-orbit or exchange fields on the Dirac states at the Fermi energy. Most importantly, due to strong SOC of $5d$ TMs, the magnitude of the QAHE gaps is increased by an order of magnitude, when compared to all QAHE systems suggested before, guaranteeing a strong topological protection against defects, structural disorder of the adatoms or thermal fluctuations, and thus opening a route to QAHE at room temperature.

To summarize, we predict that graphene decorated with $5d$ transition metals is a hybrid material displaying remarkable magnetic and topological transport properties. The strong magnetoelectric effect of these systems allows an effective manipulation of these properties by external electric fields. This effect will probably be enhanced by deposition of graphene on a ferroelectric substrate. Considering the breadth of this material class including other possible heavy adatoms, such as the $4d$ TMs or $4f$ elements, we anticipate that room temperature QAHE may become possible in these systems and we encourage intense experimental research on these systems and their properties.

*h.zhang@fz-juelich.de

[1] M. Bode, M. Heide, K. von Bergmann, P. Ferriani, S. Heinze, G. Bihlmayer, A. Kubetzka, O. Pietzsch, S. Blügel, and R. Wiesendanger, Nature (London) **447**, 190 (2007).

[2] A. Smogunov, A. Dal Corso, A. Delin, R. Weht, and E. Tosatti, Nature Nanotech. **3**, 22 (2007).

[3] N. Nagaosa, J. Sinova, S. Onoda, A. MacDonald, and N. Ong, Rev. Mod. Phys. **82**, 1539 (2010).

[4] M. König, S. Wiedmann, C. Brüne, A. Roth, H. Buhmann, L. Molenkamp, X. Qi, and S.-C. Zhang, Science **318**, 766 (2007).

[5] C. X. Liu, X.-L. Qi, X. Dai, Z. Fang, and S.-C. Zhang, Phys. Rev. Lett. **101**, 146802 (2008).

[6] R. Yu, W. Zhang, H.-J. Zhang, S.-C. Zhang, X. Dai, and Z. Fang, Science **329**, 61 (2010).

[7] M. Weisheit, S. Fähler, A. Marty, Y. Souche, C. Poinsignon, and D. Givord, Science **315**, 349 (2007).

[8] C. G. Duan, J. P. Velev, R. F. Sabirianov, Z. Zhu, J. Chu, S. S. Jaswal, and E. Y. Tsymbal, Phys. Rev. Lett. **101**, 137201 (2008).

[9] J. Rondinelli, M. Stengel, and N. Spaldin, Nature Nanotech. **3**, 46 (2007).

[10] S. Blügel, Phys. Rev. Lett. **68**, 851 (1992).

[11] Y. Mokrousov, G. Bihlmayer, S. Heinze, and S. Blügel, Phys. Rev. Lett. **96**, 147201 (2006).

[12] M. J. Piotrowski, P. Piquini, and J. L. F. Da Silva, Phys. Rev. B **81**, 155446 (2010).

[13] R. Pfandzelter, G. Steierl, and C. Rau, Phys. Rev. Lett. **74**, 3467 (1995).

[14] K. S. Novoselov, A. K. Geim, S. V. Morozov, D. Jiang, Y. Zhang, S. V. Dubonos, I. V. Grigorieva, and A. A. Firsov, Science **306**, 666 (2004).

[15] A. H. Castro Neto, F. Guinea, N. M. R. Peres, K. S. Novoselov, and A. K. Geim, Rev. Mod. Phys. **81**, 109 (2009).

[16] M. Z. Hasan and C. L. Kane, Rev. Mod. Phys. **82**, 3045 (2010).

[17] K. S. Novoselov, A. K. Geim, S. V. Morozov, D. Jiang, M. I. Katsnelson, I. V. Grigorieva, G. V. Dubonos, and A. A. Firsov, Nature (London) **438**, 197 (2005).

[18] Y. Zhang, Y. Tan, H. L. Stormer, and P. Kim, Nature (London) **438**, 201 (2005).

[19] C. L. Kane and E. J. Mele, Phys. Rev. Lett. **95**, 226801 (2005).

[20] Z. Qiao, S. A. Yang, W. Feng, W.-K. Tse, J. Ding, Y. Yao, J. Wang, and Q. Niu, Phys. Rev. B **82**, 161414(R) (2010); J. Ding, Z. Qiao, W. Feng, Y. Yao, and Q. Niu, Phys. Rev. B **84**, 195444 (2011).

[21] See Supplemental Material at http://link.aps.org/supplemental/10.1103/PhysRevLett.108.056802 for the details of calculations, values of calculated spin moments, and magnetic anisotropy energies.

[22] K. T. Chan, J. B. Neaton, and M. L. Cohen, Phys. Rev. B **77**, 235430 (2008).

[23] O. V. Yazyev and A. Pasquarello, Phys. Rev. B **82**, 045407 (2010).

[24] V. Zólomi, Á. Rusznyák, J. Kürti, and C. J. Lambert, J. Phys. Chem. C **114**, 18 548 (2010).

[25] O. Cretu, A. V. Krasheninnikov, J. A. Rodríguez-Manzo, L. Sun, R. M. Nieminen, and F. Banhart, Phys. Rev. Lett. **105**, 196102 (2010).

[26] Y. Zhang, T.-T. Tang, C. Girit, Z. Hao, M. Martin, A. Zettl, M. Crommie, Y. Ron Shen, and F. Wang, Nature (London) **459**, 820 (2009).

[27] F. Xia, D. B. Farmer, M. Lin, and P. Avouris, Nano Lett. **10**, 715 (2010).

[28] H. Zhang, M. Richter, K. Koepernik, I. Opahle, F. Tasnádi, and H. Eschrig, New J. Phys. **11**, 043007 (2009).

[29] H. Zhang, F. Freimuth, S. Blügel, Y. Mokrousov, and I. Souza, Phys. Rev. Lett. **106**, 117202 (2011).